

Power System Voltage Stability analysis with Renewable power Integration

Sinan Muhiuddeen, W M Sivakumar, Anguraja R

Abstract: The purpose of this research is to find the loading limit of a power system before hitting voltage instability and to assess the margin to voltage instability of a system consisting of a wind farm. An index called Bus Apparent Power Difference Criterion (BSDC) is used to find maximum loadable point. The measure depends on the way that in the region of the voltage collapse no extra apparent power can be delivered to the affected bus. The analysis is performed combination of wind power injection at different wind speeds and line outages in the network. In the feasibility and siting studies of wind farms the steady state analysis with network contingencies give the utility or the developer a sense of network condition upon the injection of power in the network. However, the extent of voltage stability impacted due to load growth in the system is not assessed. The research paper makes way to assess the impact on voltage stability margin with obtaining the maximum loadable point of the system and assessing the best suited bus to integrate a wind farm into the system.

Keywords : Integration, RE power, Stability, Wind

I. INTRODUCTION

Power system stability is an issue which has always received attention. However, transient angle stability is understood under power system stability. Over the years and as power systems are expanded and pushed towards their limits, other types of power system instability have come into the picture like inter area oscillations, voltage stability and frequency stability and. The problems of voltage control and stability are not new to the electrical utility industry but are now being pursued by every power system enthusiast. With growing network size along with environmental and economic pressures, the possible threat of voltage instability is becoming increasingly pronounced in power system networks. The terms voltage instability and voltage collapse are frequently used reciprocally. The voltage instability is a dynamic process wherein contrast to rotor angle (synchronous) stability, voltage dynamics mainly involves loads and the means for voltage control. Voltage instability and collapse have resulted in several major system failures or blackouts. The operation of power systems closer to their loadability limits is dictated by the needs of deregulated

electricity markets. However, due to this, voltage instability has caused several blackouts. This means that voltage stability has become a serious operational issue and is the subject of significant investigation due its importance in system security and the quality of power.

Wind energy plays a major role towards a sustainable energy future. Among the many generator types used in wind power generation, the development has advanced from fixed to variable-speed concepts. Since decades Squirrel Cage Induction Generator (SCIG) has been the backbone of wind power industry. Due to the intake of reactive power and variation in output power by the windfarm with SCIG, analysis is being carried out on impact of large-scale wind power generation on voltage stability.

II. VOLTAGE STABILITY INDEX ASSESSMENT

A. PV Curves

The slower form of voltage stability are analysed using load flow method. Simulations are made for an outage or for high load built up and load flows obtained. Besides these post-disturbance power flows, two other power flow-based methods are widely used, PV curves and VQ curves. These two methods determine steady state loadability limits (or) maximum loadable limits (or) network loadability limits which are related to voltage stability. PV curves are handy in conceptual analysis of voltage stability. In order to assess the voltage stability of a system, consider a simple radial system shown in Fig. 2.1.

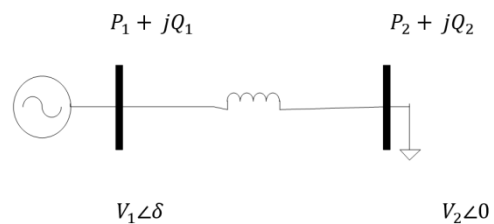


Fig 2.1: Simple radial system

Power flow at receiving end is

$$P_2 = \frac{V_1 V_2}{X} \sin \delta \quad (2.1)$$

$$Q_2 = \frac{V_1 V_2 \cos \delta - V_2^2}{X} \quad (2.2)$$

The short circuit power of the system is V_1^2 / X

Manuscript received on April 21, 2021.

Revised Manuscript received on April 28, 2021.

Manuscript published on April 30, 2021.

* Correspondence Author

Sinan M*, Department of Electrical and Electronics engineering, Don Bosco institute of technology, Bengalore, India. Email: Sinanmuhiuddeen1793@gmail.com

W M Sivakumar, Department of Electrical and Electronics engineering, Don Bosco institute of technology, Bengalore, India. Email: sssbrn7@gmail.com

Anguraja R, Department of Electrical and Electronics engineering, Don Bosco institute of technology, Bengalore, India. Email: angurajamasamy@gmail.com

Normalizing the variables based on short circuit power

$$P = \frac{P_2 X}{V_1^2} \quad (2.3)$$

$$Q = \frac{Q_2 X}{V_1^2} \quad (2.4)$$

we get

$$P = V \sin \delta \quad (2.5)$$

$$Q = V \cos \delta - V^2 \quad (2.6)$$

eliminating δ we have

$$V^4 + V^2(2Q - 1) + (P^2 + Q^2) = 0 \quad (2.7)$$

for a power factor angle ϕ

$$V^4 + V^2(2P \tan \phi - 1) + P^2 \sec^2 \phi = 0 \quad (2.8)$$

From the above equation we can draw PV curve for any power factor load.

For unity power factor

$$V^4 - V^2 + P^2 = 0 \quad (2.9)$$

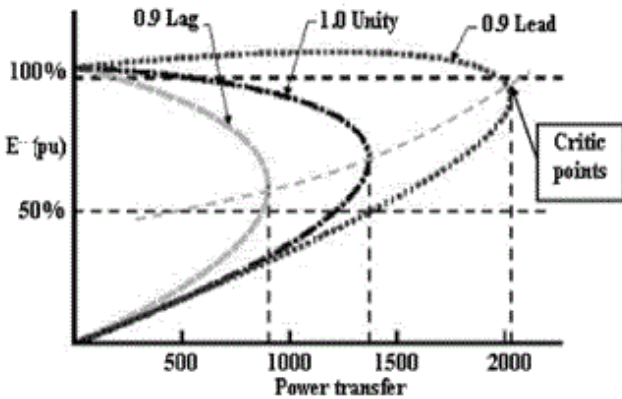


Fig A.1: Typical PV curve

B. BSDC Index

Bus Apparent power Difference Criterion (BSDC) is based on the fact that the stressed lines become consumers of huge sum of reactive power and they begin restricting the reactive power supply to a load bus in the vicinity of the voltage collapse.

This means

$$\Delta V_k \Delta I_{ki}^* = V_k \Delta I_{ki}^* + I_{ki}^* \Delta V_k + \Delta S_{ki} \quad (2.10)$$

At the point of voltage collapse, $\Delta S_{ki} = 0$

The condition $\Delta S_{ki}=0$ at the receiving end of a line results in a demand for a higher reactive-power inflow on the other lines connected to the affected bus k, and in the final step all of the connected lines fail to supply the load bus k. Consequently, no additional apparent power can be delivered to the load k. This can be formally written as

$$\Delta S_k = 0 \quad (2.11)$$

Eq.(2.12) can be further developed in a similar way

$$\Delta S_k = V_k \Delta I_k^* + I_k^* \Delta V_k + \Delta V_k \Delta I_k^* \quad (2.12)$$

Since $\Delta V_k \Delta I_k^*$ represents a very small value if a sufficiently small sample step is used, it can be neglected and eq.(2.12) can be written as:

$$\Delta S_k = V_k \Delta I_k^* + I_k^* \Delta V_k = 0 \quad (2.13)$$

$$|V_k \Delta I_k^*| = |I_k^* \Delta V_k| \quad (2.14)$$

$$\left| \frac{V_k}{I_k^*} \right| = \left| \frac{\Delta V_k}{\Delta I_k^*} \right| \quad (2.15)$$

$$BSDC = \frac{\left| \frac{V_k}{I_k^*} - \frac{\Delta V_k}{\Delta I_k^*} \right|}{\left| \frac{V_k}{I_k^*} \right|} \quad (2.16)$$

C. Modelling of wind turbine with SCIG

An induction machine that has the property to work both as induction motor and as an induction generator has two sets of windings-one on the rotor and other on the stator, but only one set actively participates in energy conversion process. Therefore, SCIG is also called a singly fed electric generator. The three-phase stator winding of the SCIG, which is symmetrically distributed along stator circumference, is connected to a balanced 3-phase source (grid). However, SCIGs are not self-exciting. They depend on an external voltage source (e.g. the electric grid) to produce a rotating magnetic field by the stator.

The interaction of the generator rotor bar currents with the rotating magnetic field in the air gap generate a tangential force on the rotor, generating a torque and causing the rotor to rotate against the direction of rotation in the generating mode. If the rotor runs at synchronous speed, there will be no stator flux, cutting the rotor, no current induced in the rotor and hence no torque. The slip between the rotor and the synchronous speed stator field develops torque. The ratio of the speed of actual flux cutting the rotor to synchronous speed is defined as slip given by

$$s = \frac{N_s - N}{N_s} \quad ,$$

where, s = slip

N_s = synchronous speed

N = rotor speed

On starting the machine as an induction motor the slip is unity, while at synchronous speed slip is zero. Slip is defined as 'negative' when the machine is running as generator which is about -1% to -2%, when used along with wind turbine.

When the wind turbine rotor (driven by wind) makes the SCIG rotor shaft speed to coincide with the stator rotating magnetic field, it no more intersects the rotor winding and no power is drawn from the grid, and rotor is said to be idling at synchronous speed, i.e. without any load.

But when the wind thrust continues to apply more torque through the wind turbine rotor to make the generator rotor run faster than the stator's rotating magnetic field, the machine is said to run at super synchronous speed, the induction machine becomes an induction generator and starts generating electric power rather than consuming it, thus returning power back to grid. The harder the wind cranks the wind turbine rotor and the generator shaft connected to it, the more electric power gets produced and pumped into the grid.

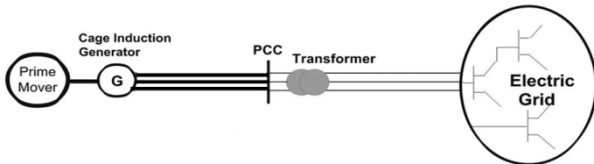


Fig C.1: Schematic diagram of SCIG connected to grid

Table I: Parameters of wind turbine considered

Parameter	Value
Rotor diameter, m	42
Hub height, m	35
Gear box ratio	1:50
Cut-in wind speed, m/s	4.5
Rated wind speed, m/s	15
Cut-out wind speed, m/s	25

Table II: Parameters of SCIG considered

Parameter	Value
Active power, kW	600
Terminal voltage, V	690
Stator Resistance, mΩ	7.10
Stator reactance, mΩ	72.3
Rotor Resistance, mΩ	5.60
Rotor reactance, mΩ	88.3
Magnetisation reactance, Ω	3.05

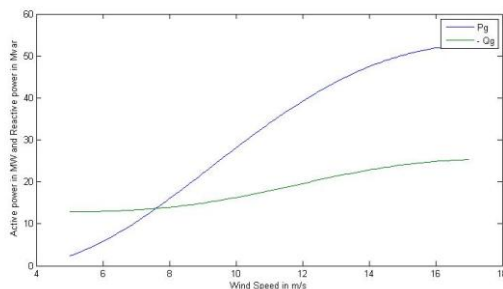


Fig C.2: Power variation of integrated windfarm

III. SIMULATION AND RESULTS

Voltage stability analysis is done on standard IEEE 5 bus system. Parameter acquisition (voltage and current phasors at the load buses) is done by using Newton Raphson Load Flow analysis. Voltage Stability Index Assessment is done by

calculating BSDC index.

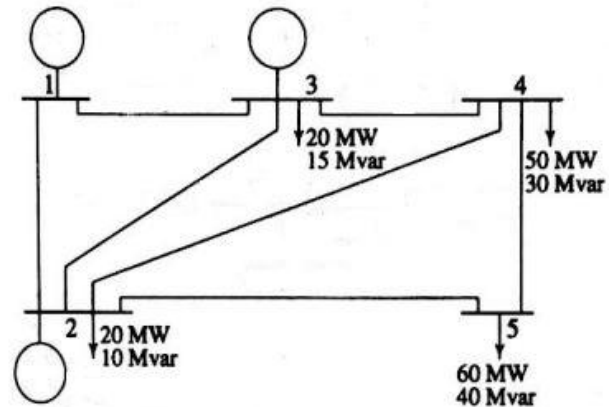


Fig C.1: Standard 5 bus system

A. Analysis with windfarm placed at bus 5 and outage of line (4-5)

Table III: Windfarm placed at bus 5 and outage of line (4-5)

Wind Speed(m/s)	Bus 4		Bus 5		Maximum LF
	Voltage in p.u.	BSDC	Voltage in p.u.	BSDC	
5	0.8140	0.1746	0.6052	0.0343	3.17
7	0.8167	0.2399	0.6172	0.0687	3.25
9	0.8057	0.1769	0.6015	0.0322	3.34
11	0.8147	0.2001	0.6216	0.0484	3.36
13	0.8361	0.2458	0.6578	0.0795	3.28
15	0.8559	0.2857	0.6878	0.1011	3.19

B. Analysis with windfarm placed at bus 5 and outage of line (2-5)

Table IV: Windfarm placed at bus 5 and outage of line (2-5)

Wind Speed(m/s)	Bus 4		Bus 5		Maximum LF
	Voltage in p.u.	BSDC	Voltage in p.u.	BSDC	
5	0.6542	0.0254	0.6918	0.1515	1.25
7	0.6131	0.0217	0.6654	0.0767	1.32
9	0.6339	0.0740	0.6852	0.1346	1.37
11	0.6429	0.0043	0.6559	0.0168	1.39
13	0.6511	0.0890	0.6946	0.1490	1.39
15	0.6661	0.0928	0.7020	0.1396	1.28

C. Analysis with windfarm placed at bus 4 and outage of line (4-5)

Table IV: Windfarm placed at bus 4 and outage of line (4-5)

Wind Speed(m/s)	Bus 4		Bus 5		Maximum LF
	Voltage in p.u.	BSDC	Voltage in p.u.	BSDC	
5	0.8077	0.1946	0.6057	0.0345	3.16
7	0.8130	0.1935	0.6097	0.0298	3.19
9	0.8165	0.2603	0.5959	0.0633	3.21
11	0.8236	0.2389	0.6186	0.0493	3.28
13	0.8226	0.2291	0.6159	0.0420	3.30
15	0.8228	0.2499	0.6200	0.0528	3.18



D. Analysis with windfarm placed at bus 4 and outage of line (2-5)

Table V: Windfarm placed at bus 4 and outage of line (2-5)

Wind Speed(m/s)	Bus 4		Bus 5		Maximum LF
	Voltage in p.u.	BSDC	Voltage in p.u.	BSDC	
5	0.6541	0.1459	0.7059	0.1988	1.27
7	0.6446	0.1191	0.6944	0.1653	1.28
9	0.6320	0.0826	0.6818	0.1225	1.30
11	0.6593	0.1468	0.7080	0.1856	1.39
13	0.6955	0.2316	0.7441	0.2717	1.42
15	0.7068	0.2348	0.7594	0.2822	1.30

In order to identify the suitable location of windfarm that provides higher loading factor over a broad range of wind velocity, the Standard Deviation (SD) of loading factor at various wind velocities is computed.

Table VI: Standard deviation of loading factor with windfarm

Placement of windfarm at load bus	SD of loading factor
4	1.207
5	1.2167

It is observed that the standard deviation is marginally less when the windfarm is placed at bus 4. Therefore, it is observed that placement of windfarm at bus 4 will make the system voltage stable over a wide range of wind velocity as compared to bus 5.

IV. CONCLUSION

Though a lot of wind farm integration studies are done with respect to the network feasibility, the margin of voltage stability with the integration of the wind farm and the variation with the load growth is not assessed and captured. Voltage stability analysis of the system with network contingencies, power injection at various wind speeds and load growth gives a better picture of the reliability, robustness and better clarity of the power system network. In the end it allows a developer or a utility to choose the best suited bus to inject the wind power considering both the network feasibility and voltage stability.

REFERENCES

1. Khoi Vu, Miroslav M. Begovic, Damir Novosel, Murari MohanSaha (1999) Use of Local Measurements to Estimate Voltage-Stability Margin. *IEEE Transactions on Power Systems*, 14, 3, 1029-1035.
2. Verbic.G, F. Gubina (2004) A new concept of voltage-collapse protection based on local phasors. *IEEE Transactions on Power Delivery*. 19, 7, 576-581.
3. Ivan Smon, Milos Pantos, Ferdinand Gubina (2008) An improved voltage-collapse protection algorithm based on local phasors. *Electric Power Systems Research*,78, 434-440.
4. Boonchiam.P.N, A.Sode-Yome, N. Mithulanathan, K.Aodsup (2009) Voltage Stability in Power Network when connected Wind Farm Generators. *International conference on Power Electronics and Drives*, Taipei, 655-660.
5. D. Devaraj, R. Jeevajyothi (2011) Impact of fixed and variable speed wind turbine systems on power system voltage stability enhancement. *IET conference on Renewable Power Generation*, Edinburgh, 1-9.

AUTHORS PROFILE



Sinan Muhiuddeen, is working as an Analyst in ICF international. He received his B.E in Electrical and electronics engineering and pursuing M.Tech in power system from VTU Belgaum. His fields of interest are power system, power quality, security constrained economic dispatch, greenfield siting for RE power development



Dr. W M Sivakumar, is working as Professor in Department of electrical and electronics engineering at Don Bosco institute of technology, Bangalore. He received his Doctorate in Artificial Intelligence Methodologies. He has 38 years of unstinted & spotless Government Service in Energy Sector. He received the first "Outstanding Engineer" Award of the Karnataka Electricity Board (KEB), Government of Karnataka, India



Dr. Anguraja R., is working as Professor and head of the department of Department of electrical and electronics engineering at Don Bosco institute of technology, Bangalore. He received his M.Tech in High voltage Engineering from SASTRA and Ph.D degree in electrical and electronics Engineering from Jain University, Bangalore. He has 22 years of academic and research experience. His fields of interest are power system, High voltage engineering and renewable energy sources.

